

# A NOVEL OPTIMIZATION APPROACH TO FICTITIOUS DOMAIN METHODS

DANIEL AGRSS AND PATRICK GUIDOTTI

ABSTRACT. A new approach to the solution of boundary value problems within the so-called *fictitious domain methods* philosophy is proposed which avoids well known shortcomings of other fictitious domain methods, including the need to generate extensions of the data. The salient feature of the novel method, which we refer to as SSEM (Smooth Selection Embedding Method), is that it reduces the whole boundary value problem to a linear constraint for an appropriate optimization problem formulated in a larger, simpler set containing the domain on which the boundary value problem is posed and which allows for the use of straightforward discretizations. The proposed method in essence computes a (discrete) extension of the solution to the boundary value problem by selecting it as a smooth element of the complete affine family of solutions of the original equations now yielding an under-determined problem for an unknown defined in the whole fictitious domain. The actual regularity of this extension is determined by that of the analytic solution and the choice of objective functional. Numerical experiments will demonstrate that it can be stably used to efficiently deal with non-constant coefficients, general geometries, and different boundary conditions in dimensions  $d = 1, 2, 3$  and that it produces solutions of tunable (and high) accuracy.

## 1. INTRODUCTION

In this paper an optimization approach is proposed for the resolution of general boundary value problems within the framework of *fictitious domain methods* (we include so-called *immersed boundary methods* in this class). While the ideas and the methods readily apply to any boundary value problem, the approach will be illustrated by means of second order boundary value problems of type

$$\begin{cases} \mathcal{A}u = f & \text{in } \Omega, \\ \mathcal{B}u = g & \text{on } \Gamma = \partial\Omega, \end{cases} \quad (1.1)$$

for an elliptic operator  $\mathcal{A}$  such as, e.g., the Laplacian  $-\Delta$ , and an admissible boundary operator  $\mathcal{B}$  such as, e.g., the trace  $\gamma_\Gamma$  (Dirichlet problem), the unit outer normal derivative  $\partial_\nu$  (Neumann problem), or a combination thereof (Robin type problem). Such boundary value problems have traditionally been strongly or weakly (when in divergence form) formulated as well-posed problems which admit a unique solution (up to a constant for some boundary conditions). Most numerical methods, reflecting this approach and viewpoint, are either a direct discretization of the problem, like in the case of finite difference methods, or the discretization of a suitable Dirichlet form-based weak formulation of the problem, like in the case of finite element methods. When the domain is special, highly accurate spectral discretizations can be utilized. The former methods come with the heavy burden of generating a mesh for the domain (this becomes a serious limiting factor when dealing with some problems, like, for instance, Moving Boundary Problems or in three space dimensions), whereas the latter are limited by the small number of allowable shapes for  $\Omega$  and lose some of their benefits for non-constant coefficients operators. Two widely used methods which seek to avoid these difficulties are known as the *fictitious domain method* and the *immersed boundary*

---

*Key words and phrases.* Fictitious domain methods, numerical solution of boundary value problems, boundary value problems as optimization problems, high order discretizations of boundary value problems.

*method.* These techniques, which we refer to simply as *embedding methods*, transplant the problem from the original domain  $\Omega$  to an encompassing simple region, where straightforward discretizations and solvers can be utilized. The approach proposed here can be viewed as a novel embedding method, which reduces the whole boundary value problem to the role of a linear constraint to an optimization problem for an appropriately chosen functional defined on the larger domain. The output of the method will coincide with an approximation of the solution of the boundary value problem in the domain  $\Omega$  and with a smooth extension of it defined on  $\mathbb{B}$ . The degree of smoothness will be determined by the data and the chosen functional. The method has the advantage of working for general domains and general data (read, non-constant coefficients and any type of boundary conditions) while delivering a paradigm to obtain, in principle, discretizations of any degree of accuracy. Not least, it allows for straightforward, robust implementation, by use of either the QR decomposition or the preconditioned conjugate gradient method (PCG). It differs from other embedding methods in that the boundary value problem is left unmodified in the extension process to the larger domain  $\mathbb{B}$ . In other words, the interior and boundary equations are simply discretized by means of the new regular grid in  $\Omega$  and on  $\partial\Omega$  for a new “extended” unknown vector defined on  $\mathbb{B}^m$  (a discretization of  $\mathbb{B}$ ). A solution is then computed by selecting a smooth element from the affine space of solutions of the under-determined problem which results from imposing the equations on the extended vector.

**1.1. Description of the method.** As the focus of this paper is on a numerical procedure, the method will be described at the discrete level. A parallel continuous formulation as well as an analysis of the method will be addressed elsewhere. The continuous counterpart, however, does provide insights that will be exploited later in the paper in the construction of effective preconditioners for the iterative PCG-based solution of the derived equations. For this reason some basic properties of the continuous operators will be mentioned here and there.

First fix a simple (square or rectangular) domain  $\mathbb{B}$  for which  $\Omega \subset \mathbb{B}$ . In this paper  $\mathbb{B}$  will be chosen to be the periodic box  $(-\pi, \pi)^d \subset \mathbb{R}^d$ . Denote by  $\mathbb{B}^m$  a regular uniform discretization of  $\mathbb{B}$  consisting of  $N_m$  points, where  $m$  is the number of discretization points along one and each dimension. Replace the continuous differential operator by a discrete counterpart  $A = A^m$ , defined as a discrete evaluation of  $\mathcal{A}$  at grid-points which lie inside  $\Omega$

$$x \in \Omega^m = \Omega \cap \mathbb{B}^m = \{x_k \mid k = 1, \dots, N_m^\Omega\}, \quad N_m^\Omega \in \mathbb{N},$$

where  $A^m$  acts on “discrete functions” defined on  $\mathbb{B}^m$ . Given a set of points

$$\Gamma^m = \{y_j \mid j = 1, \dots, N_m^\Gamma\} \subset \Gamma$$

it is possible to discretize the boundary condition using any kind of interpolation and any kind of discrete differentiation (where needed) based on the grid  $\mathbb{B}^m$  and obtain the corresponding discrete equation  $Bu = B^m u^m = g^m$  for the unknown vector  $u^m : \mathbb{B}^m \rightarrow \mathbb{R}$  and a discretization  $g^m$  of the boundary function  $g$ , defined on  $\Gamma^m$ . In this way the continuous boundary value problem (1.1) can be replaced by the discrete under-determined system given by

$$Cu = C_m u^m = \begin{bmatrix} A \\ B \end{bmatrix} u = \begin{bmatrix} A^m \\ B^m \end{bmatrix} u^m = \begin{bmatrix} f^m \\ g^m \end{bmatrix} = b^m = b \quad (1.2)$$

where  $f^m$  is a discretization of  $f$  at grid points in  $\mathbb{B}^m \cap \Omega$ . As the notation indicates, we shall often suppress the superscripts and the indices to simplify the notation. Notice that

$$u^m \in \mathbb{R}^{N_m}, \quad f^m \in \mathbb{R}^{N_m^\Omega}, \quad \text{and} \quad g^m \in \mathbb{R}^{N_m^\Gamma},$$

for  $N_m^\Omega = |\Omega \cap \mathbb{B}^m| = |\Omega^m|$ . Clearly it is always ensured that  $N_m^\Omega + N_m^\Gamma < N_m$  so that the problem, while under-determined, admits solutions. While not strictly necessary, care is also taken to make

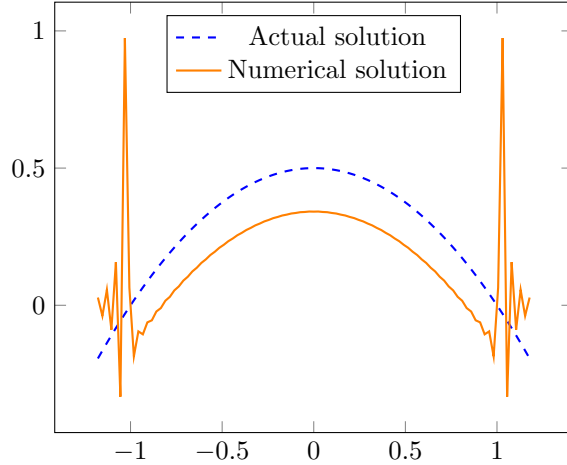


FIGURE 1. A 1D visualization of the oscillations caused by trivial extension with no regularization. The plot only shows a region that is only slightly larger than  $\Omega$  since the oscillations occur in a neighborhood of  $\partial\Omega$ .

sure that all equations in the system are independent of each other. The reason is numerical conditioning of the relevant matrices (more later). Now, and in contrast to available fictitious domain methods, we don't try to extend or modify the problem to or in the encompassing domain/grid  $\mathbb{B}/\mathbb{B}^m$ , but rather try and find “the best” among the solutions of the under-determined problem (1.2). After all, if you use high order  $\mathbb{B}^m$ -based discretizations of derivatives and evaluations, the equations should be sufficient to determine a solution that achieves their order of accuracy (up to the order allowed by the regularity of the solution itself, of course).

A simpliminded approach (which is fine when no regularity at all is expected) would now be to find a minimal norm solution of the problem, i.e. solve the linearly constrained optimization problem

$$\operatorname{argmin}_{\{Cu=b\}} \frac{1}{2} \|u\|_2^2, \quad (1.3)$$

where  $\|\cdot\|_2$  denotes the Euclidean norm on  $\mathbb{R}^{N_m}$ . This would lead to the so-called normal equations and to the solution

$$u = C^\top (CC^\top)^{-1} b.$$

Given that the matrix  $C = C_m$  consists of differential operators including the evaluation (restriction) in the domain  $\Omega^m$  and on the boundary  $\Gamma^m$ , its transpose then corresponds to differential operators containing trivial extensions (read extensions by 0) and this leads to oscillations generated by the lack of regularity. This is made apparent in Figure 1. The “good” solution is, however, among those of the under-determined problem, and can be obtained by requiring additional regularity. As already pointed out, the discretizations  $A^m$  and  $B^m$  are, after all, chosen to have a desired accuracy and the truncations/trivial extensions destroy it. Thus enforcing an appropriate degree of regularity should allow for the recovery of the intrinsic accuracy of the chosen discretizations, again, compatibly with the expected regularity of the solution itself. This is also the reason for our choice to call the proposed method Smooth Selection Embedding Method (SSEM). While this selection is done in a way that is natural from the point of view of optimization [2, Chapter 10], it has a nice analytic interpretation which will greatly help with the practical implementation of the method. Let  $\|\cdot\|_S$  be the discretization of a high order norm such as, for instance,  $\|(1 - \Delta_\pi)^{p/2} \cdot\|_2$ , where  $-\Delta_\pi$  denotes the periodic Laplacian on  $[-\pi, \pi]^d$  and  $p \geq 1$ . Now the

problem becomes

$$\operatorname{argmin}_{\{Cu=b\}} \frac{1}{2} \|u\|_S^2, \quad (1.4)$$

where the indices have again been dropped for ease of reading. The constrained optimization problem (1.4) can be reformulated as the unconstrained minimization

$$\operatorname{argmin}_{u \in \mathbb{R}^{N_m}, \Lambda \in \mathbb{R}^{N_\Lambda}} \frac{1}{2} \|u\|_S^2 + \Lambda^\top (Cu - b),$$

upon introduction of Lagrange multipliers  $\Lambda \in \mathbb{R}^{N_\Lambda}$ , where  $N_\Lambda = N_m^\Omega + N_m^\Gamma$ . A direct computation yields the regularized normal equation

$$u = S^{-1}C^\top (CS^{-1}C^\top)^{-1}b, \quad (1.5)$$

where  $S$  is the (invertible) operator corresponding to the norm  $\|\cdot\|_S$ . Now, recalling that  $C$  and  $C^\top$  are truncated differential operators (more precisely containing differentiations, evaluations on subdomains, and extensions), we see that the effect of the norm is to replace the operator  $C^\top$ , which, upon being hit by  $C$ , is the cause of the oscillations in the simpleminded method, by the smoothed  $S^{-1}C^\top$ , which can be captured numerically to a higher degree of accuracy (no oscillations) when hit by  $C$ .

**Remark 1.1.** *While, in the proposed method, Lagrange multipliers are introduced as they are in many a fictitious domain implementations, the approach is quite distinct from other methods (see below, Section 1.2.) First and foremost the Lagrange multipliers are introduced for the whole problem and not only for the purpose of satisfying the boundary condition. Secondly they are introduced naturally as an enforcement tool of a linear constraint and do not require modification of the problem, the use of extensions, or the introduction of artificial terms (often in the form of sources).*

**Remark 1.2.** *Notice that formula (1.5) can be used as a starting point without any knowledge of a norm generating the operator  $S$ . One can choose any convenient smoothing operator acting on (generalized) functions defined on the box  $\mathbb{B}$  instead of  $S^{-1}$ .*

**1.2. Comparison with Other Embedding Methods.** Particularly relevant for this paper are the so-called *fictitious domain methods* and, to a lesser degree *immersed boundary methods* and *boundary integral methods*. These alternative approaches have experienced a surge in interest in recent years and seem to be particularly popular in the applied and very applied communities. Just as with the method advocated here, the fictitious domain and immersed boundary methods avoid the mesh generation step by resorting to a “container” domain of simple geometry which admits a straightforward discretization, while boundary integral methods exploit analytical knowledge about the problem to obtain a dimensional reduction by collapsing the problem to the boundary. At the heart of any of these implementations is the need to resolve the mismatch between the boundary and the simple regular grid. There is a vast literature about these methods as they can be implemented in various discretization contexts, admit a variety of distinct practical implementations within each discretization framework, and can be applied to many different boundary value problems of mathematical physics [11]. We refer to the beginning of [10] for a brief outline of many of these methods and to [5] for a concise description/numerical implementation of a number of variants. Given the volume of publications, the choice of references made here was merely motivated by the fact that they contain a description of the methods’ philosophy and/or many useful additional references in their introduction.

**1.2.1. Fictitious Domain Methods.** A prominent implementation procedure, developed by Glowinski and coauthors in [4, 8, 7, 6] and known as the distributed Lagrange multiplier method, can be described in some more detail as follows: think of the domain  $\Omega$  as a subset of a larger regular simple domain  $\mathbb{B}$ , introduce a (uniform) discretization of  $\mathbb{B}$ , and solve the boundary value problem

by modifying the data (the right-hand-side and/or the operator  $\mathcal{A}$  in the prototypical situation considered here), usually by extending them and by introducing artificially a weighted sum of carefully chosen source terms supported outside the domain  $\Omega$ , i.e. in  $\mathbb{B} \setminus \Omega$ , or on its boundary  $\Gamma$ , by determining the weights (Lagrange multipliers) so as to make sure that the boundary condition is satisfied (or at least well-approximated). We remark that a common characteristic of these techniques (and of immersed boundary methods as well) is that Neumann or Robin boundary conditions are “natural” and straightforward to include in the formulation, whereas Dirichlet boundary conditions are more challenging (see, e.g. [5]). These methods clearly have the advantage of not requiring special care nor effort in the choice of discretization for  $\mathbb{B}$ . An often cited criticism of this approach is the need to extend the original elliptic operator  $\mathcal{A}$  and/or right-hand-side  $f$  to corresponding objects defined on the whole of  $\mathbb{B}$ . This is not always straightforward and simple minded extensions (like the trivial one by zero outside  $\Omega$ ) introduce singularities into the problem reducing the overall accuracy of the method. See [1] regarding methods of creating smooth extensions from  $\Omega$  to  $\mathbb{B}$  for the purpose of implementing fictitious domain methods. Another approach, in the context of finite elements, consists in modifying the problem’s Dirichlet form to ensure that (non-natural) boundary conditions be satisfied by possibly adding direct or more subtle penalty or penalty-like terms to it, like, e.g., the so-called Nitsche method (see [3], for example). The approach proposed here can be viewed as a novel fictitious domain method which does not require any explicit extension of the data (it can itself be used as remarked later in Section 3 to produce smooth extensions) or modification of the original boundary value problem. Moreover, it makes apparent that the real problem that any fictitious domain methods has to solve is the selection problem among the infinitely many solutions of the original problem, which are generated as the problem is viewed in a larger domain where it becomes under-determined. The direct way in which this is done here (introduction of a high order smoother) clearly shows how the order of accuracy chosen for the interior and boundary operators can be recovered in the extended problem through an affine shift obtained by a natural (both from the point of view of PDEs and of optimization) regularization.

*1.2.2. Immersed Boundary Methods.* A very popular method used to deal with complex geometries, which is one of the motivations of this paper as well, is the so-called immersed boundary method by which a problem is extended to a simple encompassing domain admitting robust and effective discretizations. The extension is obtained by the use of Dirac distributions in the distance from the boundary (more precisely, line and surface integral distributions along the boundary) and hence typically introduces singularities which reduce the overall accuracy of the method to first order. Recently, approaches have been proposed in which the accuracy is improved by the use of extension operators that preserve smoothness. We refer in particular to [12] for an immersed boundary method which includes a smooth extension method, thereby preserving higher order accuracy, albeit at the cost of significant additional computational time (in what is called the preparation phase in the paper). We again point out that the method proposed here does not require any explicit extension since it identifies the solution among the infinitely many of the extended, under-determined problem by simply requiring smoothness in the full computational domain (and hence across the boundary) along with directly enforcing the PDE in  $\Omega$  and the boundary conditions on  $\partial\Omega$  by resorting only to the regular grid.

*1.2.3. Boundary Integral Methods.* While not directly connected to boundary integral methods, the procedure developed here allows for a nice discrete interpretation of these from the point of view of optimization. They can be used when the existence of an explicit representation for a fundamental solution  $G$  of the differential operator  $\mathcal{A}$  is known. In this case one can use the representation  $u_h = \int_{\Gamma} G(\cdot, y)h(y) d\sigma_{\Gamma}(y)$  for solutions of  $\mathcal{A}u = 0$  and reduce the boundary value

problem to determining the density  $h : \Gamma \rightarrow \mathbb{R}$  such that

$$Bu_h(x) = B \int_{\Gamma} G(x, y)h(y) d\sigma_{\Gamma}(y) = g(x), \quad x \in \Gamma. \quad (1.6)$$

This effectively leads to a dimensional reduction in the problem as the unknown density function is only defined on the boundary.

In formulation (1.4), this corresponds to situations where the kernel of  $A$  is known and can therefore be represented as the range of a matrix  $M$ . In this case, if  $u_f$  is a particular solution of  $Au = f$ , then the optimization problem can be reduced to

$$\operatorname{argmin}_{\{BMz=g-Bu_f\}} \frac{1}{2} \|u_f + Mz\|_S^2, \quad (1.7)$$

for the unknown (boundary and hence smaller) vector  $z$ . While the regularization used here introduces an additional layer not present in a pure boundary integral formulation, the corresponding problem can also be efficiently solved given the explicit nature of the smoother and of the encompassing domain. Clearly  $M$  corresponds to the integral operator appearing in (1.6), while  $B$  is the continuous boundary operator in (1.6) and a corresponding discretization of it in (1.7).

**Remarks 1.3.** *We conclude this introduction with a few important remarks.*

(a) *The method is generic in the sense that it does not require specific discretizations of the encompassing domain  $\mathbb{B}$  and of the data. It is rather a procedure that can be adapted to the context of finite differences, finite elements, or spectral methods quite easily.*

(b) *It has the structure of a classical optimization problem with linear constraints for which a host of methods exists which can be used for its resolution. While there seem to be “natural” choices for the smoothing norm  $\|\cdot\|_S$ , it is possible to work with other (non-quadratic) functionals, that may deliver better results for specific problems.*

(c) *It fully avoids the issues related to the need of generating extensions of the data from the domain  $\Omega$  to the encompassing box  $\mathbb{B}$ , while, as a matter of fact, it can itself be adapted to produce smooth extensions. See Section 3 later in this paper.*

(d) *As the numerical experiments presented in Section 4 will demonstrate, it is general enough to be robustly implemented for general domains, for non-constant coefficients, as well as for a variety of problems (in divergence form and not) and boundary conditions. In its high order implementations, it clearly heavily relies on the smoothness of the data (and hence of the solution), but can be used for non smooth problems as well (see Section 4.4). Clearly even better results can be obtained in this case, if specific attention is paid to the region in which the solution is singular by, e.g., introducing a weighted smoothing norm.*

## 2. METHOD

**2.1. Methods for Solving the Linear System.** Before we turn to describing the actual discretizations of the domain and the differential operators, we describe two general methods for solving the linear system in such a way as to obtain a solution of high accuracy. As described in Section 1.1, the boundary value problem can be reduced to finding

$$\operatorname{argmin}_{u \in \mathbb{R}^{N_m}, \Lambda \in \mathbb{R}^{N_\Lambda}} \frac{1}{2} \|u\|_{S_p}^2 + \Lambda^\top (Cu - b).$$

Here,  $\|\cdot\|_{S_p}^2 = \|(1 - \Delta_\pi)^{p/2} \cdot\|^2$  is a penalty norm introduced to enforce the regularity of the solution across the boundary. Thus, the penalty term imposes the  $H_\pi^p(\overline{\mathbb{B}})$  regularity of the solution (if at all available; but  $p$  can and will of course be adapted to the solution). The subscript  $\pi$  indicates periodicity. This form of the problem can then be reduced to computing the regularized normal equation

$$u = S_p^{-1} C^\top (C S_p^{-1} C^\top)^{-1} b,$$

where the operator  $S_p$  is given by

$$S_p u = (1 - \Delta_\pi)^p u.$$

A naive approach to solving this linear system would be to directly invert the (regularized) normal matrix  $CS_p^{-1}C^T$ . However, such an approach fails to produce a solution of high accuracy. To obtain such a solution, it is necessary to either use

- a smoother with  $p$  very large to obtain a very fast rate of convergence, or
- a very dense grid, where even a slowly converging solution can converge.

Directly inverting the matrix fails in both of these approaches. Clearly, for a dense grid, particularly in three dimensions, it becomes prohibitively expensive to store and directly invert the normal matrix  $CS_p^{-1}C^T$ . On the other hand, the order  $p$  of the smoother can not be pushed too high without hitting the limits of numerical precision. We recall that the smoother is given by  $(1 - \Delta_\pi)^{-p}$ . In Fourier space, this corresponds to a multiplication by the function  $(1 + |k|^2)^{-p}$ . If  $k_*$  is largest mode, as soon as  $|k|_*^{-2p}$  drops below machine precision, which is roughly  $1e - 16$ , some matrix entries can no longer be captured numerically and the benefits of accuracy are lost. For example, on a grid of size  $64^2$ , the highest order smoother which can be used is  $p = 5$ . This greatly limits the accuracy we can obtain.

To remedy these problems, we propose two solutions. The first continues to use explicit matrices, but uses a QR decomposition to increase the maximal effective  $p$ . The second uses an iterative solver, the PCG method, which relies on an implicit form of the linear operator rather than an explicit matrix, to allow for solving the system on larger grids.

2.1.1. *QR Approach.* We consider the QR decomposition of the matrix

$$S_p^{-1/2}C^T = QR.$$

Here, using the notation of Section 1.1,  $Q \in \mathbb{R}^{N_m \times N_\Lambda}$  is an orthogonal matrix satisfying  $Q^T Q = I$  while  $R \in \mathbb{R}^{N_\Lambda \times N_\Lambda}$  is an upper triangular matrix. We then calculate that

$$\begin{aligned} S_p^{-1}C^T(CS_p^{-1}C^T)^{-1} &= S_p^{-1/2}QR(R^T Q^T QR)^{-1} \\ &= S_p^{-1/2}QRR^{-1}(R^T)^{-1} \\ &= S_p^{-1/2}Q(R^T)^{-1}. \end{aligned}$$

What makes this method effective is that the  $RR^{-1}$  cancellation reduces the power  $S_p^{-1}$  in the matrix to  $S_p^{-1/2}$ . Thus, we are able to double the order  $2p$  of the smoother before the onset of machine precision limitations. We are therefore able to use any  $p \leq 10$  and obtain a highly accurate solution for a coarse grid very efficiently, as demonstrated by the numerical experiment documented in Figure 2 and Table 1.

2.1.2. *Using the PCG method.* An alternative approach consists in using an iterative solver to deal with the linear system on very dense grids. As discussed earlier, numerical limitations will allow us to only use such a method with a smoother of limited order ( $p \leq 4$ ). However, by increasing the grid size, we are able to compensate for the smaller order and still obtain an accurate solution. Because the linear operators  $C$ ,  $C^T$ , and  $S_p^{-1}$  can be naturally implemented using sparse matrices (in the case of finite difference discretizations) or the FFT (in the case of spectral discretizations), iterative methods will lend themselves to very fast computation. Furthermore, the matrix is positive and symmetric, so a natural candidate is the conjugate gradient method. We note  $S_p$  is of order  $-2p$ . Thus, it will be very ill-conditioned for large grids and good preconditioning is necessary. We refer to Section 2.4 for a more detailed description of the preconditioning procedure which allows for an efficient PCG implementation. We note, however, that the preconditioning is more effective for the lower order smoothers; thus, the increased accuracy stemming from the use of  $S_4$  needs to be balanced against the larger condition number, and hence the slower convergence relative

to  $S_2$  and  $S_3$  for a given grid size. We note that the  $S_2$  has the particular advantage that, with the preconditioning discussed in Section 2.4, the condition number of the corresponding operator remains uniformly bounded, regardless of grid size. This is because the operator  $C$  is second order in the interior. As  $S_2^{-1}$  is of order  $-4$ ,  $CS_2^{-1}C^T$  is of order 0 in the interior. In Table 2.4, we show the growth in condition number for  $S_2, S_3$ , and  $S_4$  for the discretization of the disc problem described in Section 2.2.

**2.1.3. Rates of convergence and contrasting the methods.** Next we describe the effectiveness of each of the QR and PCG methods, and discuss when each should be used. As described in the introduction, a smoother  $S_p$  seeks to find an  $H_\pi^p(\overline{\mathbb{B}})$  extension of the solution. Thus, whenever the true solution is smooth, we expect that the rate of convergence of the discrete solution will be of order  $p$ . In Figure 2, we demonstrate the rate of convergence of various order smoothers using both the QR and PCG methods. The problem studied is posed on the disc  $D$  of radius 1 and reads

$$\begin{cases} -\Delta u = -3(x - y) & \text{in } D, \\ u = x^3 - y^3 & \text{on } \partial D. \end{cases} \quad (2.8)$$

The exact solution is  $x^3 - y^3$ . The figure clearly shows the  $p$  rate of convergence for each smoother. We note that the  $L_\infty$  error converges similarly. Clearly, for a smooth problem, the higher order QR method on a course grid outperforms the PCG method, even on a denser grid. However, in less favorable cases, the PCG method may be advantageous. For example, for very irregular boundaries, a dense grid may be necessary to resolve their geometry and the PCG method may be necessary. Similarly, if the solution itself is not regular, the higher order smoothers will not achieve faster convergence and it may be necessary to use the PCG method on a denser grid. Notice, however, that use of an SVD decomposition on a dense grid is still possible by using a library which accepts an implicit linear operator rather than an explicit matrix as its input. This would be an alternative which preserves the accuracy of the QR method with the larger grid of implicit methods.

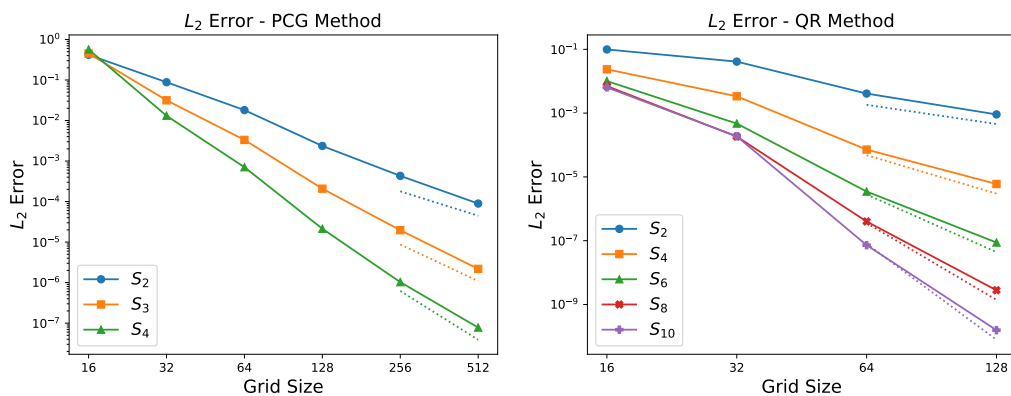


FIGURE 2. Convergence of the  $L_2$  error for different order smoothers solving Equation 2.8. The light dotted lines are reference lines of slope  $\frac{1}{m^p}$  where  $m$  is the number of grid points along one dimension.



Grid Size	CPU Times - PCG Method			CPU Times - QR Method				
	$S_2$	$S_3$	$S_4$	$S_2$	$S_4$	$S_6$	$S_8$	$S_{10}$
$16^2$	0.01	0.01	0.01	0.15	0.19	0.17	0.21	0.18
$32^2$	0.01	0.02	0.03	0.17	0.23	0.2	0.24	0.23
$64^2$	0.01	0.03	0.07	0.39	0.56	0.52	0.56	0.61
$128^2$	0.04	0.13	0.54	6.61	7.96	8.01	8.62	7.95
$256^2$	0.33	0.59	2.75					
$512^2$	2.15	4.32	24.07					

TABLE 1. CPU times for solving Equation 2.8. All computations were performed on an Intel 7700HQ.

**2.2. Discretization of the Domain.** As described in the introduction, we begin by embedding the domain  $\Omega$  into a torus  $\mathbb{B}$  in order to make use of spectral methods and of the Fourier transform. The periodicity box  $\mathbb{B}$  is discretized with a uniform grid  $\mathbb{B}^m$ . The boundary  $\Gamma$  is approximated with a discretization  $\Gamma^m$ , which is just a set of  $N_m^\Gamma$  points lying on  $\partial\Omega$ . In practice, it is best for these points to be uniformly distributed across the boundary. In two dimensions, this can be accomplished easily by equally spacing points along an arc length parametrization of the curve. In three dimensions, equally distributing the points around a surface is more challenging, although well known algorithms exist for placing points on  $S^2$ . In Section 4.5, we use the well known Fibonacci algorithm (see [9]) to create a discretization.

A choice also needs to be made concerning the density of boundary points, that is, the value of  $n$ . When using an insufficient number of points on the boundary, the accuracy suffers, while too many points can drive up the condition number. When using the QR implementation, the method is relatively immune to ill conditioning, since explicit matrices are used. Thus the boundary points can be placed close together. If  $m$  is the number of grid points along one dimension, a density of  $\frac{1}{2} \frac{m}{2\pi}$  boundary points per unit length seems to be effective. The PCG iterative method, on the other hand, is quite sensitive to ill-conditioning of the matrix. It turns out to be more effective to space the points further apart according to a density of  $\frac{1}{4} \frac{m}{2\pi}$  points per unit length. This guarantees that three to four regular grid points lie between any two boundary points and thereby allows the regular grid  $\mathbb{B}^m$  to easily "distinguish" the different boundary points, thereby keeping the condition number relatively low. In Figure 3, we show the discretization of a disc  $D$  with the first density described, and a star shaped domain with the second. For better visualization, we have only plotted the region  $[-1.3, 1.3]^2$ , as opposed to the entire region  $[-\pi, \pi]^2$ . In three dimensional problems, we have found that with a grid of size  $m^3$  points, a boundary spacing of  $2 \left(\frac{m}{2\pi}\right)^2$  per unit area for the QR method is most effective, while  $\frac{1}{16} \left(\frac{m}{2\pi}\right)^2$  per unit area is best for the PCG method. This smaller density maintains three to four box discretization points between each boundary point along each dimension, allowing the regular box grid to resolve the "irregular" boundary discretization grid.

**2.3. Discretizing the Differential Operators.** We now discuss the discretization of the differential operators  $C, C^\top$ , and  $S_p$ .

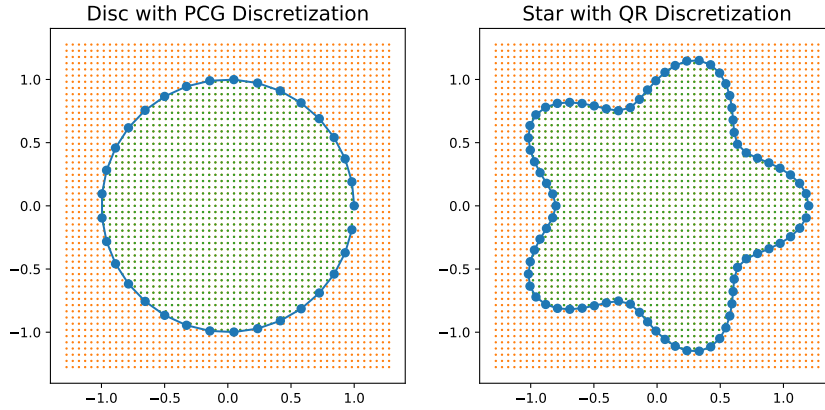


FIGURE 3. Discretizing the boundary.

2.3.1. *Discretization of  $C$  and  $C^\top$* . We recall that

$$C = \begin{pmatrix} A^m \\ B^m \end{pmatrix},$$

where  $A^m$  is a matrix of evaluations of a second order differential operator at the points found in the set  $\Omega^m = \mathbb{B}^m \cap \Omega$ , and  $B^m$  is a matrix of evaluations of a boundary operator on the finite subset  $\Gamma^m$  of  $\partial\Omega$ . We begin by evaluating any necessary derivatives on the entire domain  $\mathbb{B}^m$ . As discussed in the introduction, the purpose of using a fictitious domain method is that it allows us to easily use techniques which apply to the torus, and extend them to problems with more complex geometries. In particular, the partial derivatives can be calculated using either finite difference methods or spectral methods on the torus. Spectral methods have the advantage of delivering greater accuracy for smooth problems, while finite difference methods have the advantage of being slightly faster and being more readily applicable to a wider range of differential operators. Once the partial derivatives have been calculated, we restrict the results to  $\Omega^m$  and multiply by the coefficients of the operator  $A^m$ .

In all of the numerical experiments below, we evaluate the derivatives used for the operator  $A^m$  spectrally. More specifically, whenever taking the Laplacian, we compute

$$(-\Delta)^m = (\mathcal{F}^m)^{-1} \text{diag}\left(\left(|k|^2\right)_{k \in \mathbb{Z}_m^d}\right) \mathcal{F}^m,$$

where  $\mathcal{F}^m$  is the discrete fast Fourier transform and  $k \in \mathbb{Z}_m^d$  is the frequency vector at discretization level  $m$ . In Subsection 4.1, where we examine nonconstant coefficients, we similarly use the Fourier transform to evaluate the second derivatives in each combination of directions. However, we would like to reiterate that  $A^m$  can be implemented with any numerical scheme for calculating derivatives on the torus. The choices we made were simply dictated by convenience. Spectral methods are used because we wish to demonstrate the high order of accuracy which can be obtained by the proposed method.

When applying  $(A^m)^\top$ , we begin by multiplying by the coefficient of  $A^m$  and, then, take the transpose of the restriction operator part of  $A^m$ , which amounts to an extension by 0 outside of  $\Omega^m$ . In this way, we are able to use the chosen method to evaluate the derivatives.

Because the boundary points  $\Gamma^m$  do not lie on the regular grid, we need to use interpolation operators when implementing the boundary operator  $B^m$ . Given that we are interpolating from a

regular rectangular grid, the interpolation operators are simple. Linear, cubic, or spectral interpolation can all be used. In the examples below, we have used spectral interpolation. This is because, as mentioned earlier, we wish to demonstrate the high order of convergence of the method.

**Remark 2.1.** *The rate of convergence of the solution is constrained by the order of the smoother, the interpolation operators, and the differential operators. To avoid wasting computational resources, the order of accuracy of these various discretizations should be made to match. If the expected regularity of the solution is known, it can also be taken into consideration when making this choice.*

2.3.2. *Discretizing the Smoother  $S_p$ .* We now discuss the discretization of the smoother

$$S_p u = (1 - \Delta_\pi)^p u.$$

Because the operator  $S_p$  is defined over the torus  $\overline{\mathbb{B}}$ , we are able to use the fast Fourier transform to calculate  $S_p^{-1}$ , or, as when using the QR method,  $S_p^{-1/2}$ . We define the matrix  $S_p$  with diagonal entries

$$(S_p)_{kk} = (1 + |k|^2)^p,$$

where  $k \in \mathbb{Z}_m^d$  is the vector of frequencies. We then note that

$$S_p^{-1} b = (\mathcal{F}^m)^{-1} S_p^{-1} \mathcal{F}^m b.$$

Using the fast Fourier transform, this operator can be evaluated efficiently with minimal memory requirements.

2.3.3. *Calculating the Explicit Matrices.* When using the PCG method, the matrix multiplication can be evaluated implicitly and there is no need to explicitly calculate the matrix entries. However, the QR decomposition requires an explicit matrix representation for  $C^\top S_p^{-1/2}$ . In our implementation, we have used the simplest option of generating the matrix columns by column by evaluating  $C^\top S_p^{-1/2} e_i$  for  $1 \leq i \leq N_\Lambda$  for the natural basis vectors  $e_i$ . Although this entails many evaluations of the matrix, for sparse grids, this time cost is small and the method is still very efficient.

An alternative method would be to exploit the fact that the derivative operators and the smoothing operators are cyclic on the regular grid. Thus, the matrix can easily be calculated by simply shifting, for example,  $S_p^{-1/2} e_1$  around the grid. A drawback, however, this method entails explicitly calculating the larger matrix  $S_p^{-1/2}$  which can use large amounts of RAM. We emphasize that the times quoted in the tables include the time required to calculate the explicit matrices. We also point out again that libraries exist which can take the SVD decomposition implicitly; while using the SVD decomposition is slower than the QR decomposition, doing so would eliminate the need for the evaluation step.

2.4. **Preconditioning and PCG Implementation.** We now return to a more detailed discussion of the implementation of the PCG method. As discussed in 2.1.2, the normal matrix  $C S_p^{-1} C^\top$  is very ill-conditioned and requires a good preconditioner to be inverted using iterative methods. We note that the ill-conditioning occurs because of the high order of the operator and because the boundary operator and the interior operator have different orders. To demonstrate this, we think of the operator  $C S_p^{-1} C^\top$  as a block matrix

$$C S_p^{-1} C^\top = \begin{pmatrix} A^m S_p^{-1} (A^m)^\top & A^m S_p^{-1} (B^m)^\top \\ B^n S_p^{-1} (A^m)^\top & B^n S_p^{-1} (B^m)^\top \end{pmatrix} = \begin{pmatrix} C_1 & C_2 \\ C_2^\top & C_3 \end{pmatrix}.$$

As  $S_p^{-1}$  is an operator of order  $-2p$ , the matrix  $C_1$  is of order  $4 - 2p$ ,  $C_2$  is of order  $2 - 2p$  and  $C_3$  is of order  $-2p$  (for a boundary operator of order 0). In general, if an operator is of order  $-2p$ , the condition number of its matrix will grow like a polynomial of degree  $2p$  as the grid size increases

(for example, on a grid of size  $m$ , the largest eigenvalue of the Laplace operator will be of size  $m^2$ ). Thus, the large order together with the mismatch in scaling causes a very large condition number. We will describe a simple preconditioner which works effectively for  $S_2$ ,  $S_3$ , and  $S_4$ . The preconditioning consists of finding approximate inverses to the  $C_1$  and  $C_3$  blocks independently. The general philosophy consists in preconditioning the operator so that it becomes order 0.

We begin by finding an approximate inverse for the  $C_3$  block. In the following description, we will consider a Dirichlet problem, where the boundary operator  $\mathcal{B}$  consists of evaluation on the boundary. The discrete boundary points belonging to  $\Gamma^m$  will be denoted by  $y_i$  for  $1 \leq i \leq N_m^\Gamma$ . We recall that

$$B^m : \mathbb{R}^{\mathbb{B}^m} \rightarrow \mathbb{R}^{\Gamma^m} \text{ and } S_p : \mathbb{R}^{\mathbb{B}^m} \rightarrow \mathbb{R}^{\mathbb{B}^m}.$$

We now consider the operators

$$\tilde{B}^m : C(\mathbb{B}) \rightarrow \mathbb{R}^{\Gamma^m} \text{ where } [\tilde{B}^m u]_i = \langle \delta_{y_i}, u \rangle = u(y_i)$$

and

$$\tilde{S}_p : H_\pi^{2p-d/2-\varepsilon}(\mathbb{B}) \rightarrow H_\pi^{-d/2-\varepsilon}(\mathbb{B}) \text{ where } \tilde{S}_p u = (1 - \Delta_\pi)^p u.$$

We note that  $\tilde{B}^m$  and  $\tilde{S}_p$  can be viewed as approximations of  $B^m$  and  $S_p$  respectively, operating on the continuous  $\mathbb{B}$  rather than the discrete  $\mathbb{B}^m$ . The integral operator

$$\tilde{C}_3 := \tilde{B}^m \tilde{S}_p^{-1} (\tilde{B}^m)^T : \mathbb{R}^{\Gamma^m} \rightarrow \mathbb{R}^{\Gamma^m} \text{ with kernel } [\tilde{C}_3]_{ij} = \langle \delta_{y_i}, \tilde{S}_p^{-1} \delta_{y_j} \rangle, \quad 1 \leq i, j \leq N_m^\Gamma,$$

is then a good approximation of  $C_3$ . Notice that  $\delta_y \in H_\pi^{-d/2-\varepsilon}(\mathbb{B})$  for any  $y \in \mathbb{B}$  and  $\varepsilon > 0$ . If we define

$$h(y) = \left( \tilde{S}_p^{-1} \delta \right) (y)$$

as the fundamental solution of  $\tilde{S}_p$  on the torus  $\mathbb{B}$ , we find, by translation invariance of the torus, that

$$[\tilde{C}_3]_{ij} = \left( \frac{2\pi}{m} \right)^d h(y_i - y_j).$$

Here, by an abuse of notation, the factor  $\left( \frac{2\pi}{m} \right)^d$  is built-in to account for the fact that the “matrix”  $\tilde{C}_3$  acts as an integral operator and not as simply matrix-vector multiplication. Given a good value table for  $h$ , we can easily calculate the matrix  $\tilde{C}_3$  by evaluating the function  $h$  on the matrix of differences between the points in  $\Gamma^m$ . Given the explicit matrix  $\tilde{C}_3$ , we can directly calculate  $(\tilde{C}_3)^{-1}$  and use it as a preconditioner for the  $C_3$  block of the matrix. Although this entails inverting a dense matrix, for coarse grids in three dimensions and even for very fine grids in two dimensions, the number of boundary points is small enough that inverting, storing, and applying the matrix is computationally negligible.

To calculate the function  $h$ , several methods can be used. In our implementation, we proceed as follows. We take  $\tilde{m}$  large and generate a very fine grid of size  $\tilde{m}^d$  on the torus  $\mathbb{B}$ . In our examples, we used  $\tilde{m} = 4096$ . We define the vector  $\delta^{\tilde{m}}$  by

$$\delta_k^{\tilde{m}} = \begin{cases} \frac{\tilde{m}^d}{(2\pi)^d}, & \text{if } k = 0, \\ 0, & \text{otherwise.} \end{cases}$$

The vector  $\delta^{\tilde{m}}$  is then an approximation of the continuous (periodic)  $\delta$  distribution supported in the origin. We then compute  $S_p^{-1} \delta^{\tilde{m}}$  on the fine grid. This function is a good approximation of  $h$  evaluated at the points  $\mathbb{B}^{\tilde{m}}$ . We use cubic interpolation to evaluate  $h$  at points which do not lie in  $\mathbb{B}^{\tilde{m}}$ . In order to reduce RAM requirements, we only store the numerical values of  $h$  computed by means of the  $4096^2$  ( $512^3$  in dimension 3) on a smaller  $256^d$  grid. It is also beneficial to store these values in memory so they do not need to be recalculated for each problem.

For the Neumann problem, we note that the order of the matrix  $C_3$  is decreased by 2, because  $C$  and  $C^\top$  both evaluate one derivative on the boundary. Thus, rather than using the function  $S_p^{-1}\delta$ , we instead use the function  $S_{p-1}^{-1}\delta$ . See Section 4.3 for the effect of this preconditioning for the Neumann problem.

We now turn to finding an approximate inverse to  $C_1$ . The matrix  $C_1$  depends on the order of the smoother we have chosen. For  $S_2$ , we note that the matrix  $C_1$  is of order 0. Thus, no preconditioning is necessary, and  $\tilde{C}_1^{-1}$  can be taken as the identity. For the  $S_3$  and  $S_4$ , we note that the operator  $C_1$  is the discretization of a differential operator of order  $4 - 2p$ . We wish to precondition in such a way as to reduce the order of the operator to order 0. Thus, we define the preconditioner

$$\tilde{C}_1^{-1}u = (1 - \Delta_\Omega)^{\frac{2p-4}{2}}u.$$

Here,  $\Delta_\Omega$  is the Laplace operator on  $\Omega$ . In order to implement it, we use the domain discretization  $\Omega^m = \mathbb{B}^m \cap \Omega$  and a finite difference scheme to discretize the Laplacian on  $\Omega^m$ . In the examples the five points stencil (seven points in three dimensions) was chosen to take the Laplacian on  $\Omega^m$ . With this preconditioner

$$\tilde{C}^{-1} = \begin{pmatrix} \tilde{C}_1^{-1} & 0 \\ 0 & \tilde{C}_3^{-1} \end{pmatrix},$$

the condition number of the preconditioned normal matrix  $\tilde{C}^{-1/2}(CS_p^{-1}C^\top)\tilde{C}^{-1/2}$  stays uniformly bounded, independent of grid size when  $p = 2$ . When  $p = 3$ , its condition number grows slightly with grid size, while when  $p = 4$ , it grows significantly with grid size; we refer to Table 2.4. Despite this growth, however, the method is quite efficient; see Table 1 as well as the experiments in Section 4 for CPU times.

Grid Points	Boundary Points	Condition Number			PCG Iterations		
		$S_2$	$S_3$	$S_4$	$S_2$	$S_3$	$S_4$
$16 \times 16$	5	4	17	61	12	20	24
$32 \times 32$	9	6	20	80	17	30	46
$64 \times 64$	17	6	23	151	19	33	62
$128 \times 128$	33	8	25	303	20	37	81
$256 \times 256$	65	7	25	596	20	33	121

TABLE 2. Condition numbers and number of iterations for the PCG method solving Equation 2.8. The condition number is that of the preconditioned normal matrix  $\tilde{C}^{-1/2}(CS_p^{-1}C^\top)\tilde{C}^{-1/2}$ .

### 3. EXTENSION PROBLEMS

As described in the introduction, a common problem that is encountered when embedding a problem with complex geometry in a container space is the (smooth) extension of some or all of the data from the original domain to the encompassing one. We briefly outline how the proposed method can be used to generate periodic  $H_\pi^p(\mathbb{B})$  extensions to the torus. Other boundary conditions on  $\mathbb{B}$  can also be used, of course, with the appropriate modifications. In this paper we stick to the periodic setting.

The extension problem consists of finding  $\tilde{u} \in H_\pi^p(\mathbb{B})$ , given a domain  $\Omega \subset \mathbb{B}$  as well as a function  $u \in H^p(\Omega)$ , satisfying  $\tilde{u}|_\Omega = u$ . Following the spirit of the proposed method, we begin

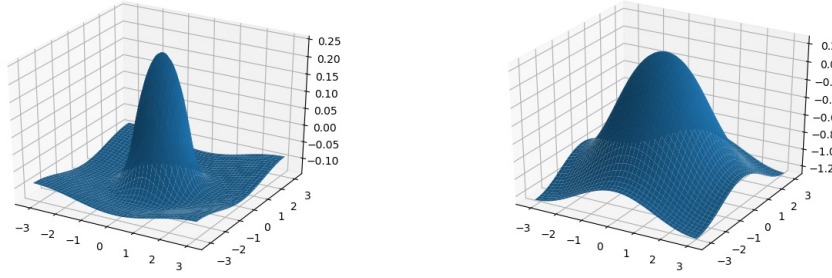


FIGURE 4.  $S_2$  and  $S_4$  extensions of  $\frac{1}{4}(1-r^2)$ .

by taking a regular discretization  $\mathbb{B}^m$  of  $\mathbb{B}$ . We then define the operator  $C$  to be the restriction to  $\Omega^m = \Omega \cap \mathbb{B}^m$ . Correspondingly  $C^\top$  is simply given by the extension by 0 from  $\Omega^m$  to  $\mathbb{B}^m$ . Finally we look for  $\tilde{u}$  which minimizes the energy defined as

$$\operatorname{argmin}_{u \in \mathbb{R}^{N_m}, \Lambda \in \mathbb{R}^{N_\Lambda}} \frac{1}{2} \|u\|_{S_p}^2 + \Lambda^\top (Cu - b),$$

As above, we take  $\|u\|_{S_p}^2 = \|(1 - \Delta_\pi)^p u\|^2$ . The problem reduces to the regularized normal equation

$$u = S_p^{-1} C^\top (C S_p^{-1} C^\top)^{-1} b. \quad (3.9)$$

The linear system can then be solved using either the QR method or the PCG method, as described in Section 2. We remark that the different extensions resulting from the different choice of  $p$  used in the smoother will produce functions of a very different nature, as they are minimizing different powers of the Laplacian; which power  $p$  is optimal will depend on the application which the extension is being used for.

Next let's look at an example. Let  $\Omega$  be the unit disc. We will produce an extension of the function

$$u|_\Omega = \frac{1}{4}(1-r^2).$$

We do this by setting  $S_p u = (1 - \Delta_\pi)^p u$ , where  $p = 2, 4$ . The construction of  $S_p^{-1}$  is the same as in Section 2.3.2. The result of the extension done on a  $128^2$  grid using the two smoothers are shown in Figure 4 with a graph and in Figure 5 as a contour plot. In Table 3, we show how the different smoothers affect different Sobolev seminorms of the corresponding minimizers.

Smoother	$\ \nabla^2 u\ _{L_2}$	$\ \nabla^3 u\ _{L_2}$	$\ \nabla^4 u\ _{L_2}$
$S_2$	1.99	11.47	169.24
$S_4$	2.84	3.42	6.45

TABLE 3. Gradient seminorms for the extension operator with  $u = \frac{1}{4}(1-r^2)$  on a grid of size  $128^2$ .

#### 4. NUMERICAL EXPERIMENTS

In the numerical experiments of this section, we solve the relevant system using both the QR and PCG methods following the procedure described in Section 2. We will then record the  $L_2$

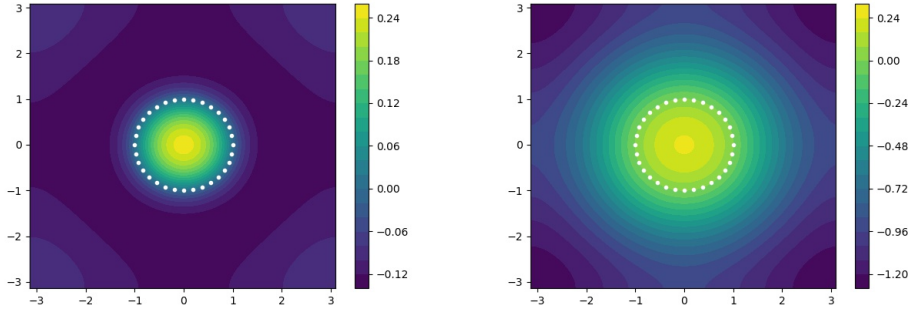


FIGURE 5.  $S_2$  and  $S_4$  extensions of  $\frac{1}{4}(1 - r^2)$ . The white dots show the discrete boundary between  $\Omega$  and the fictitious domain.

errors and the CPU times for each. We consider problems with nonconstant coefficients, with complex geometry, with Neumann boundary and with nonsmooth boundary conditions. For last we solve a three dimensional problem with  $\Omega = B^3$ , the ball of radius 1.

**4.1. Nonconstant Coefficients.** Let  $\Omega$  be the unit disc  $D$  discretized as described in 2.2 and study the problem

$$\begin{cases} -\left[(2+y)\partial_x^2 + (2-x)\partial_y^2\right]u = -6x(2+y) + 6y(2-x) & D, \\ u = x^3 - y^3 & \text{on } \partial D. \end{cases} \quad (4.10)$$

The exact solution is  $x^3 - y^3$ . The solution is calculated using the methodology described in Section 2. Comparing Figures 2 and 6, we see that the accuracy achieved is roughly equivalent for both the constant coefficient problem and the nonconstant coefficient problem. Comparing Table 4 with Table 1, we see that the QR method CPU time is comparable to the constant coefficient case, whereas the PCG method is considerably slower. Clearly, the condition number of the matrix grows faster for the nonconstant coefficient problem. However, both methods are still robust enough to efficiently solve nonconstant coefficient problems.

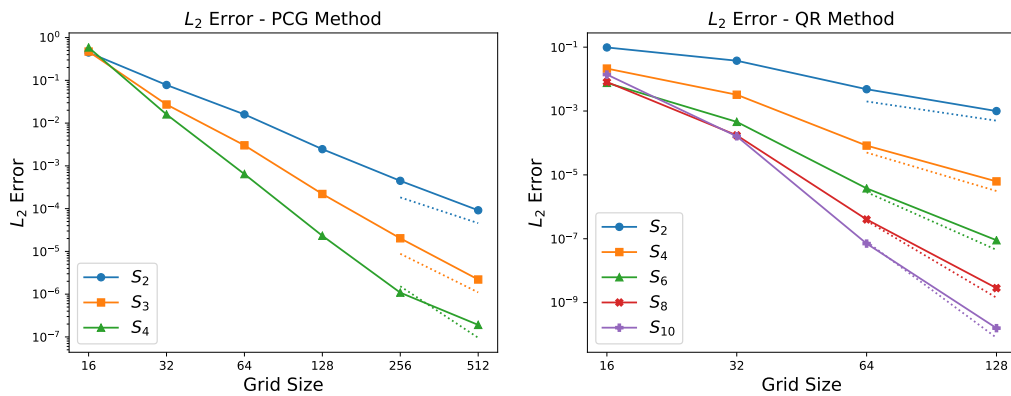


FIGURE 6. Convergence of the  $L_2$  error for different order smoothers solving Equation 4.10. The light dotted lines are reference lines of slope  $\frac{1}{m^p}$  where  $m$  is the number of grid points along one dimension.

Grid Size	CPU Times - PCG Method			CPU Times - QR Method				
	$S_2$	$S_3$	$S_4$	$S_2$	$S_4$	$S_6$	$S_8$	$S_{10}$
$16^2$	0.24	0.29	0.29	0.01	0.01	0.01	0.01	0.01
$32^2$	0.27	0.33	0.39	0.05	0.05	0.06	0.06	0.06
$64^2$	0.3	0.4	0.46	0.32	0.45	0.44	0.47	0.45
$128^2$	0.52	0.68	0.93	7.5	9.0	9.26	9.41	9.76
$256^2$	1.95	2.67	5.94					
$512^2$	11.13	14.51	48.15					

TABLE 4. CPU times for solving Equation 4.10. All computations were performed on an Intel 7700HQ.

4.2. **A Flower Shaped Domain.** For a problem on a more complex domain, we consider a five petaled flower.

$$\Omega = \{(r, \theta) \mid r < 1 + .2 \cos(5\theta)\}.$$

Figure 3 shows  $\Omega$  with its boundary discretization. We solve the problem

$$\begin{cases} -\Delta u = 0 & \text{in } \Omega, \\ u = x^2 - y^2 & \text{on } \partial\Omega \end{cases} \quad (4.11)$$

The exact solution is  $x^2 - y^2$ . The results of this experiment, contained in Figure 7 and Table 5, demonstrate that the accuracy and efficiency of the method is maintained even for a complex geometry. We note, however, that the PCG method is somewhat slower to converge on the flower than the disc. We believe that, given the complexity of the shape, boundary points are necessarily closer together and therefore more difficult for the interior grid to resolve.

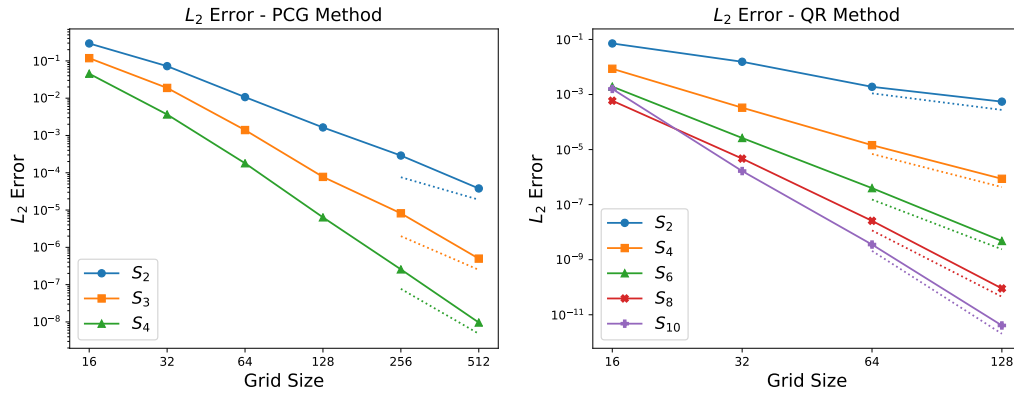


FIGURE 7. Convergence of the  $L_2$  error for different order smoothers solving Equation 4.11. The light dotted lines are reference lines of slope  $\frac{1}{m^p}$  where  $m$  is the number of grid points along one dimension.



Grid Size	CPU Times - PCG Method			CPU Times - QR Method				
	$S_2$	$S_3$	$S_4$	$S_2$	$S_4$	$S_6$	$S_8$	$S_{10}$
$16^2$	0.27	0.25	0.26	0.23	0.21	0.16	0.17	0.17
$32^2$	0.29	0.29	0.32	0.22	0.2	0.19	0.22	0.21
$64^2$	0.37	0.39	0.46	0.47	0.54	0.54	0.54	0.54
$128^2$	0.51	0.98	1.56	7.44	8.34	8.3	8.29	9.1
$256^2$	1.51	3.54	16.48					
$512^2$	8.39	23.78	205.56					

TABLE 5. CPU times for solving Equation 4.11. All computations were performed on an Intel 7700HQ.

**4.3. Neumann Boundary Conditions.** In order to demonstrate how the method is also applicable to other boundary conditions, a Neumann problem is considered. We again set  $\Omega$  as the unit disc. We solve the Neumann problem

$$\begin{cases} -\Delta u = 0 & \text{in } \Omega, \\ \frac{\partial u}{\partial \nu} = 2(x^2 - y^2) & \text{on } \partial\Omega. \end{cases} \quad (4.12)$$

The exact solution is  $x^2 - y^2$ . As discussed in Section 2, we evaluate the normal derivative with a spectral interpolation. We subtract  $u(0,0)$  to eliminate the constant functions in the kernel. The convergence results are displayed in Figure 8, and the CPU times are recorded in Table 6.

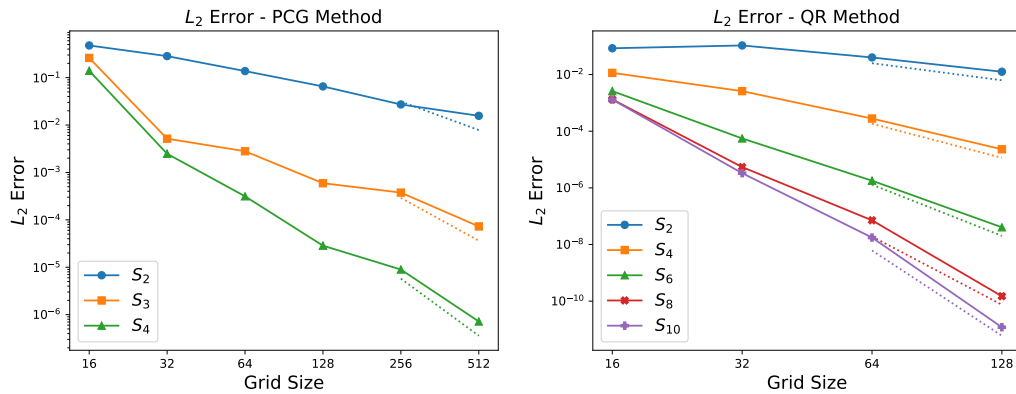


FIGURE 8. Convergence of the  $L_2$  error for different order smoothers solving Equation 4.12. The light dotted lines are reference lines of slope  $\frac{1}{m^p}$  where  $m$  is the number of grid points along one dimension.

Grid Size	CPU Times - PCG Method			CPU Times - QR Method				
	$S_2$	$S_3$	$S_4$	$S_2$	$S_4$	$S_6$	$S_8$	$S_{10}$
$16^2$	0.22	0.23	0.22	0.14	0.16	0.16	0.17	0.17
$32^2$	0.23	0.27	0.27	0.17	0.23	0.21	0.2	0.25
$64^2$	0.26	0.28	0.31	0.36	0.56	0.51	0.5	0.55
$128^2$	0.42	0.42	0.61	6.51	8.15	7.96	8.14	8.09
$256^2$	1.23	1.5	3.29					
$512^2$	6.43	8.32	31.67					

TABLE 6. CPU times for solving Equation 4.12. All computations were performed on an Intel 7700HQ.

**4.4. Non-regular Problem.** Although our method is by its nature more suited to smooth problems, it is not strictly limited to them. While the method in its current form has no hope of properly approximating the solution in the immediate vicinity of a singularity, outside a small ball containing the singularity, it converges reasonably well to the solution. In the following example, we let  $\Omega$  be the unit disc and study the nonsmooth problem

$$\begin{cases} -\Delta u = 0 & \text{in } \Omega, \\ u = g & \text{on } \partial\Omega, \end{cases}$$

where

$$g(\theta) = \begin{cases} 1 & \text{if } 0 \leq \theta \leq \pi \\ -1 & \text{if } \pi \leq \theta \leq 2\pi \end{cases}$$

in polar coordinates. In solving this problem, we will use the same discretization of the domain and operators used in the example studied in Section 2. We note that the higher order smoothers do not provide an advantage when the solution itself is not smooth, so we restrict ourselves to  $S_2$ . The true solution of this boundary value problem can be given in the form of the series

$$u(r, \theta) = \sum_{k=1}^{\infty} g_k r^k \sin(k\theta),$$

where the Fourier coefficients  $g_k$  are defined by

$$g_k = \begin{cases} \frac{4}{k\pi} & \text{if } k \text{ is odd,} \\ 0 & \text{if } k \text{ is even.} \end{cases}$$

The two singularities occur at  $y_1 = [1, 0]$  and  $y_2 = [-1, 0]$ . We will study the solution away from the singularities in two ways. First, we will look at the  $L_2$  error on  $\tilde{\Omega} = \Omega \setminus (B(y_1, 0.2) \cup B(y_2, 0.2))$ , which cuts out the singularities. The region  $\tilde{\Omega}$  and the corresponding errors are shown in Figure 9. The graph show a convergence rate of approximately 1.5. We also show the approximated solution along the curve  $r = .9$ ,  $0 \leq \theta \leq \pi$  in Figure 10. As the grid becomes more dense, the approximations get closer to the true solution.

We also would like to point out that the general framework of our method could potentially be modified to allow it to deal with singular problems more effectively; this could either be done by allowing an adaptive grid which is more dense in the region of the singularity or by modifying

the norm used to generate the smoother  $S^{-1}$  by introducing weights or allowing for some singular behavior.

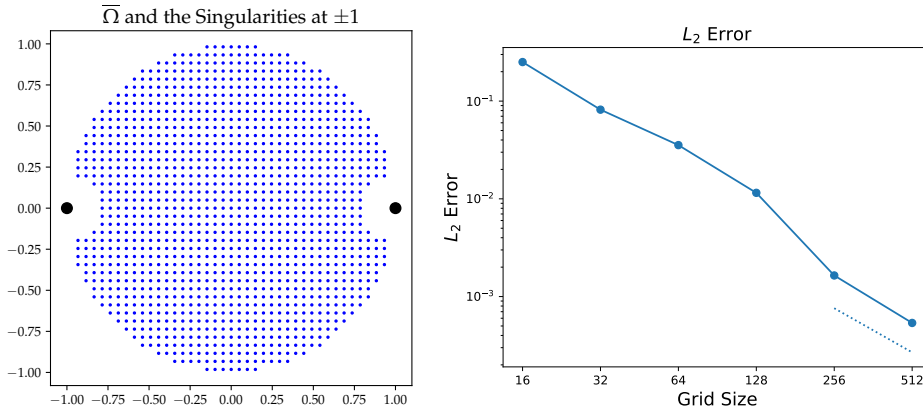


FIGURE 9. The domain  $\bar{\Omega}$  and the convergence of the nonregular problem away from the singularities. The reference line is slope  $(\frac{1}{m})^{1.5}$ , where  $m$  is the number of grid points along one dimension.

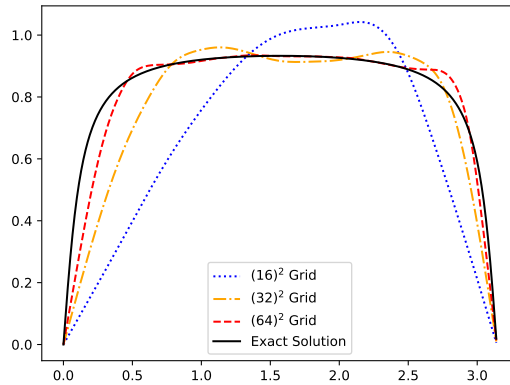


FIGURE 10. Values of the approximated solution along the curve  $r = .9$ .

**4.5. The Sphere.** For a three dimensional example, we choose the unit sphere embedded in the three dimensional torus. The boundary is discretized by the well known Fibonacci lattice [9] which comes close to distributing points uniformly on the sphere. With a box discretization of  $m^3$  points, we use  $\frac{1}{16} (\frac{m}{2\pi})^2$  in the QR method and  $\frac{1}{16} (\frac{m}{2\pi})^2$  boundary points in the PCG method; see Section 2.2 for a more detailed discussion. The problem considered is

$$\begin{cases} -\Delta u = 1 & \text{in } \Omega, \\ u = 0 & \text{on } \partial\Omega. \end{cases} \quad (4.13)$$

The exact solution is  $\frac{1-r^2}{6}$ . We see in Figure 11 that the rate of convergence achieved is similar to that of the two dimensional problem. Obviously, given the larger dimension, the CPU times are significantly larger than in two dimensions; however, the method is still quite fast. We note that

because we are calculating explicit matrices for the QR factorization, RAM limitations prevented us from using a grid larger than  $48^3$ .

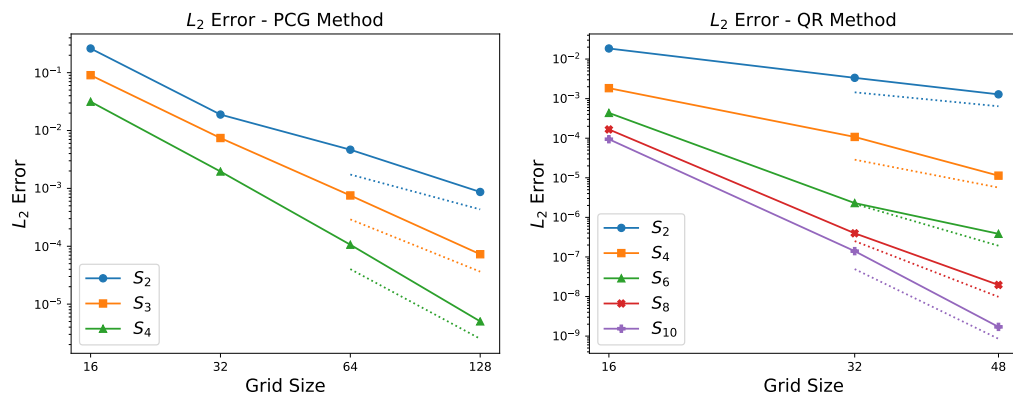


FIGURE 11. Convergence of the  $L_2$  error for different order smoothers solving Equation 4.13. The light dotted lines are reference lines of slope  $\frac{1}{m^p}$  where  $m$  is the number of grid points along one dimension.

Grid Size	CPU Times - PCG Method			CPU Times - QR Method				
	$S_2$	$S_3$	$S_4$	$S_2$	$S_4$	$S_6$	$S_8$	$S_{10}$
$16^3$	0.02	0.12	0.06	0.23	0.25	0.35	0.29	0.29
$32^3$	0.09	0.16	0.33	9.08	12.07	11.04	11.51	11.5
$48^3$	0.44	0.70	1.44	189.78	196.58	175.58	182.03	185.81
$64^3$	1.51	2.81	5.96					
$128^3$	11.54	22.11	161.78					

TABLE 7. CPU times for solving Equation 4.13. All computations were performed on an Intel 7700HQ.

#### REFERENCES

- [1] J. P. Boyd. Fourier embedded domain methods: extending a function defined on an irregular region to a rectangle so that the extension is spatially periodic and  $C^\infty$ . *Applied Mathematics and Computation*, 161(2):591–597, 2005.
- [2] S. Boyd and L Vandenberghe. *Convex Optimization*. Cambridge University Press, 2004.
- [3] E. Burman and P. Hansbo. Fictitious domain finite element methods using cut elements: II. A stabilized Nitsche method. *Applied Numerical Mathematics*, 62(4):328–341, 2012.
- [4] E. J. Dean, Q. V. Dinh, R. Glowinski, J. He, T. W. Pan, and J. Périaux. Least squares/domain imbedding methods for Neumann problems: Applications to fluid dynamics. In *Fifth Internat. Symposium on Domain Decomposition Methods for Partial Differential Equations*, pages 451–475, 1992.
- [5] S. Del Pino and O. Pironneau. A fictitious domain based general PDE solver. *Numerical Methods for Scientific Computing Variational Problems and Applications, Barcelona*, 2003.
- [6] R. Glowinski and Q. He. A least-squares/fictitious domain method for linear elliptic problems with Robin boundary conditions. *Communications in Computational Physics*, 9(3):587–606, 2011.
- [7] R. Glowinski and Y. Kuznetsov. Distributed Lagrange multipliers based on fictitious domain method for second order elliptic problems. *Computer Methods in Applied Mechanics and Engineering*, 196(8):1498–1506, 2007.

- [8] R. Glowinski, T. W. Pan, and J. Périaux. A fictitious domain method for Dirichlet problem and applications. *Computer Methods in Applied Mechanics and Engineering*, 111(3-4):283–303, 1994.
- [9] Á. González. Measurement of areas on a sphere using Fibonacci and latitude–longitude lattices. *Mathematical Geosciences*, 42(1):42–49, 2010.
- [10] X. Li, J. Lowengrub, A. Rätz, and A. Voigt. Solving PDEs in complex geometries: a diffuse domain approach. *Communications in Mathematical Sciences*, 7(1):81–107, 2009.
- [11] R. Mittal and G. Iaccarino. Immersed boundary methods. *Annu. Rev. Fluid Mech.*, 37:239–261, 2005.
- [12] D. B. Stein, R. D. Guy, and B. Thomases. Immersed boundary smooth extension: A high-order method for solving PDE on arbitrary smooth domains using Fourier spectral methods. *Journal of Computational Physics*, 304:252–274, 2016.

UNIVERSITY OF CALIFORNIA, IRVINE, DEPARTMENT OF MATHEMATICS, 340 ROWLAND HALL, IRVINE, CA 92697-3875, USA

*E-mail address:* `dagress@uci.edu` and `gpatrick@math.uci.edu`